

A MST algorithm for source detection in γ -ray images

Riccardo Campana,^{1*} Enrico Massaro,^{1,2*} Dario Gasparrini,^{2,3,4} Sara Cutini,^{2,3,4} and Andrea Tramacere⁵

¹ Department of Physics, University of Rome “La Sapienza”, Piazzale A. Moro 2, I-00185, Rome, Italy

² ASI Science Data Center (ASDC), c/o ESRIN, Via G. Galilei, I-00044, Frascati, Italy

³ Department of Physics, University of Perugia, Via A. Pascoli, I-06123, Perugia, Italy

⁴ INAF personnell resident at ASDC under ASI contract I/024/05/1

⁵ Stanford Linear Accelerator Center, 2575 Sand Hill Road, Menlo Park, CA-94025, USA

Accepted 2007 October 19. Received 2007 September 25; in original form 2007 June 05.

ABSTRACT

We developed a source detection algorithm based on the Minimal Spanning Tree (MST), that is a graph-theoretical method useful for finding clusters in a given set of points. This algorithm is applied to γ -ray bidimensional images where the points correspond to the arrival direction of photons, and the possible sources are associated with the regions where they clusterize. Some filters to select these clusters and to reduce the spurious detections are introduced. An empirical study of the statistical properties of MST on random fields is carried in order to derive some criteria to estimate the best filter values. We introduce also two parameters useful to verify the goodness of candidate sources. To show how the MST algorithm works in the practice, we present an application to an EGRET observation of the Virgo field, at high galactic latitude and with a low and rather uniform background, in which several sources are detected.

Key words: gamma rays: observations – methods: data analysis

1 INTRODUCTION

Telescopes for satellite-based high energy γ -ray astronomy detect individual photons by means of the electron-positron pair that they generate through the detector. From the pair trajectories it is possible to reconstruct the original direction of the photon with an uncertainty that decreases with the energy, from a few degrees below 100 MeV to less than a degree above 1 GeV. This technique was applied to the past γ -ray observatories SAS-2 (Fichtel et al. 1975), COS-B (Bennett 1990) and EGRET-CGRO (Kanbach et al. 1988; Thompson et al. 1993), all equipped with spark chambers. Pair tracking is also used in the current AGILE mission (Tavani et al. 2006) and in the LAT telescope on board the next GLAST mission, both employing silicon microstrip detectors (Gehrels et al. 1999). The resulting product is an image where each photon is associated with a direction in the sky: discrete sources thus correspond to regions in which a number of photons higher than those found in the surroundings are observed. When the size of this region is consistent with the instrumental Point Spread Function the source is con-

sidered as point-like, otherwise it can be extended or a group of near sources.

Various algorithms are applied to the detection of point-like or extended sources in γ -ray astronomy: the most extensively used one is based on the Maximum Likelihood (Mattox et al. 1996), whereas others based on Wavelet Transform analysis (Damiani et al. 1997), Optimal Filter (Sanz et al. 2001), Scale-Adaptive Filter (Herranz et al. 2002), etc., were variously applied to real and simulated data to study their performances. Some of them are based on deconvolution techniques of the instrumental Point Spread Function (PSF). Many methods work directly on the pixelated images, i.e. count or intensity maps. Other methods search for clusters in the arrival directions of photon that, if statistically significant, are considered an indication of a source.

The approach considered by us is essentially a cluster search based on a *minimal spanning tree* (MST) algorithm. This technique has its root in graph theory, and highlights the *topological* pattern of connectedness of the detected photons. Given a graph $G(V, E)$, where V is the set of vertices (or *nodes*) and E is the set of weighted *edges* connecting them, a MST (Kruskal 1956; Prim 1957; Zahn 1971) is the tree (a subgraph of G without closed circuits) that connects all the points with the minimum total weight, defined as the sum of the weight of each tree’s edge. In a data set con-

* E-mail addresses: riccardo.campana@uniroma1.it and enrico.massaro@uniroma1.it

sisting of points in a Cartesian frame of reference, we can consider them as the nodes of a graph, the edges being the lines joining the nodes, weighted by their length.

The MST method was originally proposed for γ -ray source detection by Di Gesù and Sacco (1983), who investigated also the statistical properties in uniform fields. This work was developed by Di Gesù and Maccarone (1986), and De Biase et al. (1986) applied MST for detecting extended sources in EXOSAT X-ray images. Other authors applied MST methods to the goal of finding galaxy clusters, both in 2 and 3-dimensional surveys and simulations (Barrow et al. 1985; Bhavsar & Ling 1988a,b; Plionis et al. 1992; Krzevina & Saslaw 1996, Doroshkevich et al. 2001, 2004) and showed the capabilities of the method as a filament-finding algorithm.

In this paper we investigate the MST approach in γ -ray source detection, and present a new study of its statistical properties and the definition of selection criteria. We also introduce some parameters useful to classify the reliability of detected clusters to be associated with source candidates. We would like to emphasize here that this method is not *alternative* to other source detection algorithms, but it is *complementary*, in the sense that it can give a list of possible candidate sources (identified via their photons' clusterization properties) that could be further investigated by other means.

This paper is structured as follows. In Sect. 2 we describe our MST algorithm, and in Sect. 3 and 4 we investigate by means of numerical simulations the statistical distributions of edge length and node number, and we introduce some criteria useful for the source detection with our method. An example of application to an EGRET field is shown in Sect. 5, while in Sect. 6 we summarize and discuss our results.

2 THE MST ALGORITHM

The result of an observation performed by a γ -ray telescope is a photon list containing for each event the arrival direction coordinates, time, energy, and other useful parameters. Celestial coordinates (Right Ascension and Declination) of every photon define a point in a bi-dimensional frame and it can be considered a node in the graph. The edge weight λ is the angular distance between a couple of nodes.

The simplest way to find the MST of the field is a version of the Prim algorithm (also known as DJP algorithm; Prim 1957): it starts from an arbitrary selected node, finds the nearest neighbour and connects them with an edge: this is the first edge of the MST. Then it finds the point that is the nearest to any point that is already connected in the MST. After $N - 1$ iterations, where N is the total number of points, the complete MST is found. Faster and computationally optimized algorithms can be found using other theoretical properties of the MST, like being a subset of the Delaunay triangulation of the graph (Delaunay 1934). In particular, we used a fast code for the MST computation that is freely available from BOOST¹ and CGAL² libraries.

Once found the MST, to extract *only* the locations where the photon clusterize, i.e. the possible sources, and to evaluate the residual photon background, the following operations must be performed:

- **Separation:** remove all the edges having λ greater than a selected separation value Λ_c . Usually, it is chosen in units of the mean edge length Λ_m in the MST. As a result we obtain a set of disconnected sub-trees.
- **Elimination:** remove all the sub-trees having a number of nodes N_n less than or equal to a threshold value N_c . This filter is useful to remove small casual clusters of nodes, leaving only the clusters that have a high probability to be genuine sources.

After the application of these filters, the remaining sub-trees correspond to possible sources. An estimate of the source position is obtained by computing the centroid of the sub-tree nodes (i.e. the mean value of the Right Ascension and Declination between all points in the sub-tree). A refined source position can be found by computing the centroid of all the points lying inside the circle centered on the previous calculated sub-tree centroid with a radius equal to the distance of the farthest point in the sub-tree, to take into account also possible photons belonging to the source but accidentally filtered out.

An example of this procedure is shown in Fig. 1, where the upper-left panel shows a frame containing $N_{\text{tot}} = 500$ points within a square region of unit length: two clusters having different numbers of points have been added to a random generated point distribution. The first one, representative of a “strong” source, has 80 points spread on a Gaussian circle of $\sigma = 0.1$, the second one, the “faint” source, has 20 points distributed in a similar circle. The random “background” has thus 400 points. The upper-right panel shows the MST that connects all the points. In the lower-left panel are shown the clusters detected after separation with $\Lambda_c = 1.3 \Lambda_m$ and elimination with $N_c = 7$. In this case a few small size clusters are detected, which disappear when more appropriate filters are used ($\Lambda_c = \Lambda_m$, $N_c = 10$, lower-right panel), whereas the two genuine sources remain. Their positions, computed from the sub-tree centroids, have a distance smaller than 0.01 from the right ones, confirming the validity of this method to evaluate the source coordinates.

The two major points of the MST source detection are therefore the choice of the two filtering parameters and the methods to evaluate the significance of the residual sub-trees.

3 MST STATISTICAL PROPERTIES

3.1 The length distribution in the MST

According to Barrow et al. (1985), an useful criterion to distinguish a random (Poissonian) field from a field with some sources, is the shape of the frequency distribution of the edge length in the MST. These authors suggest that for a random field this distribution has an approximate Gaussian shape peaked around the mean edge length Λ_m . We studied this distribution, whose statistical properties are useful to choose the best filtering parameters. In Fig. 2 we present the frequency distributions of $x = \lambda/\Lambda_m$ computed for a frame

¹ <http://www.boost.org>

² <http://www.cgal.org>

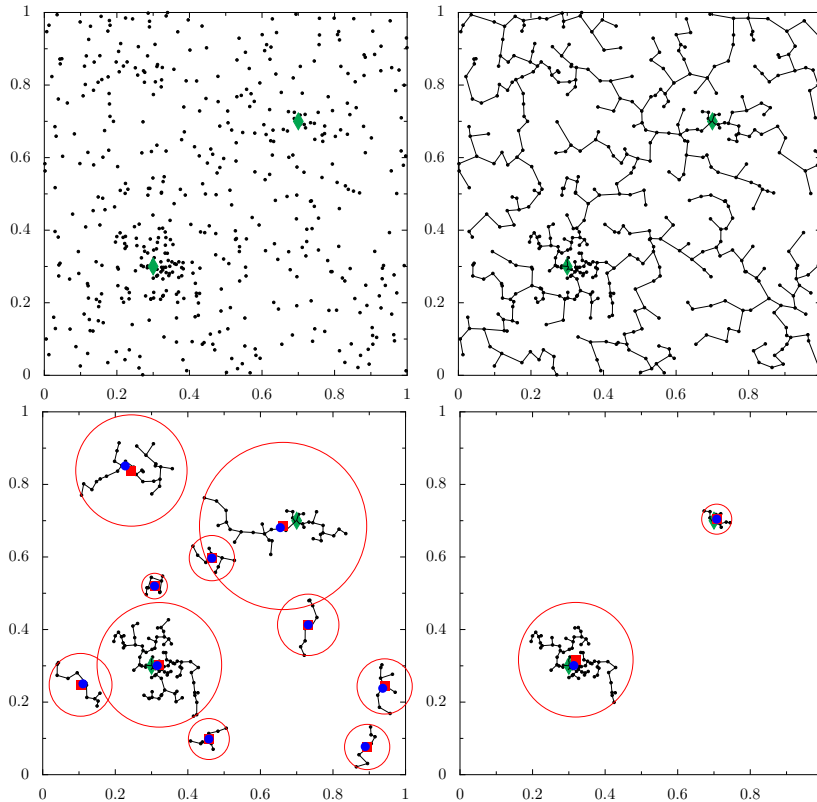


Figure 1. *Upper left:* A set of 500 random-generated points, with two simulated sources. *Upper right:* The Minimal Spanning Tree between these points. *Lower left:* Cluster selection after separation with $\Lambda_c = 1.3 \Lambda_m$ and elimination with $N_c = 7$. *Lower right:* cluster selection with the filters $\Lambda_c = \Lambda_m$, $N_c = 10$. The added “sources”, at coordinates (0.3, 0.3) and (0.7, 0.7), are marked by the diamond. Circles are centered on the centroids of the remaining sub-trees (square) and have a radii equal to the distance of the farthest node in the sub-tree. The dot is the refined source position, see text for details.

with a random field (upper panel) and the same frame with five sources added (lower panel): in the latter case there is a clear excess of short distances (within the clusters that mark the sources) and of long distances (between the clusters) with respect to the random case, and the histogram shows an evident left asymmetry.

A useful indicator for the presence of sources is the mean value of the MST length Λ_m . Earlier investigations (Gilbert 1965) found that the total length of a random MST is proportional to $\sqrt{AN_{\text{tot}}}$ where A is the field area and N_{tot} is the total number of points. A theoretical upper limit to the proportionality constant was found to be $2^{-1/2} \simeq 0.70$. Our Monte Carlo simulations showed that the constant value is rather $\simeq 0.65$. Therefore the mean length for a random-field MST is:

$$\Lambda_m \simeq 0.65 \times \sqrt{\frac{A}{N_{\text{tot}}}} \quad (1)$$

Thus, if the mean length for a field deviates from this value, it is an indicator of non-random clusterization, i.e. of the presence of sources.

Another test for the occurrence of sources is the evaluation of the skewness coefficient β_3 of the distribution $f(x)$. In the two cases of Fig. 2 we found β_3 equal to 0.16 and 0.46; the higher value is due to the decrease of the mean length Λ_m and to the occurrence of x values greater than $\simeq 2.5$ when sources are present. From our simulations we

found that β_3 higher than ~ 0.2 can be considered a good indicator for the presence of sources.

For an accurate study of the edge length distribution it is useful to have a simple analytical formula to be applied in the computation. Since theoretical works on this subject are not easily available in the astronomical literature, we followed a numerical approach.

First we generated a pure random frame containing 10^6 points to smooth the fluctuations in the histogram and the resulting frequency plot is given in Fig. 3. Note that, like in Fig. 2, it has a well defined mode, a small skewness and very small tail for $x > 2$. Its shape is not, therefore, that of a Gaussian and an approximate formula that gives an excellent best fit, although properly it is defined in the unlimited interval $[0, +\infty)$, is a Rayleigh distribution, suppressed at large x by a factor similar to that of a Fermi-Dirac (FD) distribution:

$$f(x) = K \frac{x}{\sigma^2} \exp\left\{-\frac{(x-\mu)^2}{2\sigma^2}\right\} \cdot \frac{1}{\exp\left(\frac{x-\epsilon}{d}\right) + 1} \quad (2)$$

The parameters values were found by means of a numerical best fit and the resulting formula is:

$$f(x) = \frac{5}{3} x \exp\left\{-\frac{(x+0.3)^2}{2.16}\right\} \cdot \frac{1}{\exp\left(\frac{x-1.81}{0.156}\right) + 1} \quad (3)$$

with a maximum error with respect to the data less than 2%.

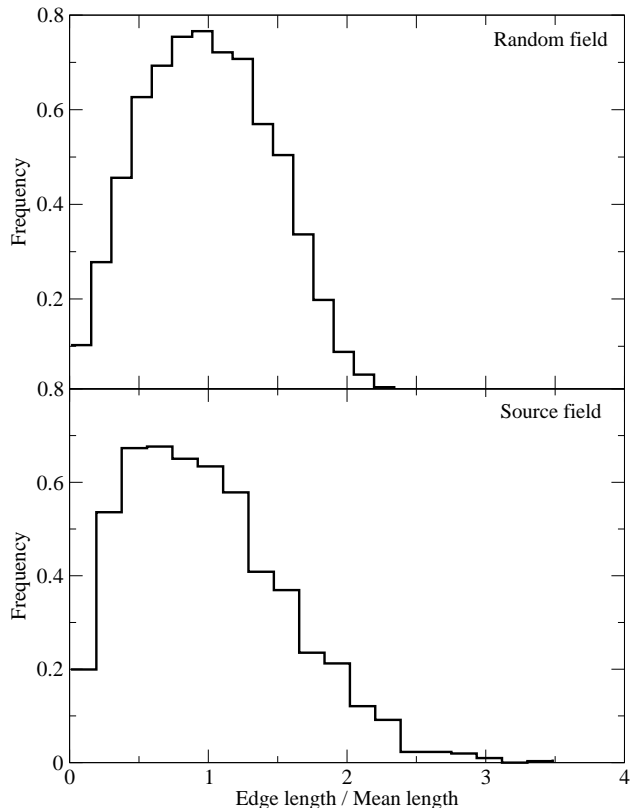


Figure 2. *Upper panel:* Histogram of the MST edge length, in units of the mean length, for a random field with 1675 points. *Lower panel:* Histogram of the MST edge length, in units of the mean length, for the same field in which some strong sources have been added. Note that there is a large left-side asymmetry with respect to the random field.

We computed the values of the mode, the median, the variance and other moments from this distribution, and found 0.892 and 0.952 respectively for the first two, a variance equal to 0.208, whereas the skewness and the kurtosis are 0.080 and 2.439, respectively.

Another fitting formula can be obtained from Pearson distributions (Smart 1958, chap. 7), again suppressed at large x values by a FD factor:

$$f(x) = K \left[\left(\frac{x}{a_1} \right)^{ba_1} \right] \left[\left(1 + \frac{a_1}{a_2} - \frac{x}{a_2} \right)^{ba_2} \right] \cdot \frac{1}{\exp\left(\frac{x-c}{d}\right) + 1} \quad (4)$$

where K is a normalization factor, a_1 is the value of the mode, b and a_2 are free parameters, c is the cut-off scale. Differently from Eq. (2), this distribution is defined in the finite interval $x \in [0, a_1 + a_2]$. Considering that values of x larger than 3.0 are extremely rare, we imposed the condition $a_1 + a_2 = 3.2$ and evaluated the remaining parameters. A very good fit was obtained for $a_1 = 0.91$, $b = 1.25$, $c = 1.8$, $d = 0.18$ and the normalisation factor $K = 0.7676$.

The edge distribution can be useful for the choice of the separation parameter Λ_c . From Eq. (3) and Figure 3, we can see that the choice of a low $X_c = \Lambda_c/\Lambda_m$, for instance the value of 0.37, implies that about 90% of edges will be

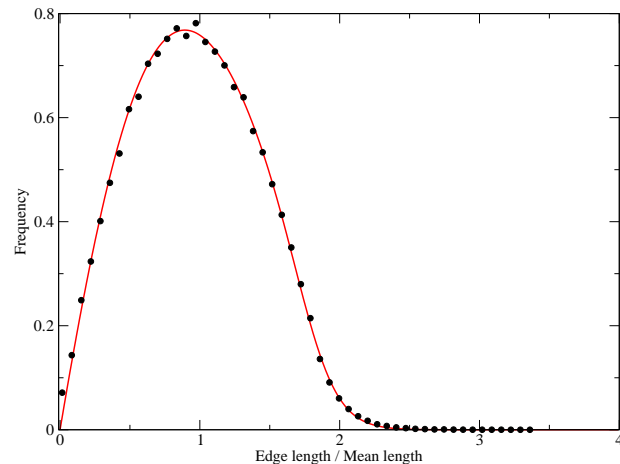


Figure 3. Histogram of the MST edge length frequency, in units of the mean length, for a random field with 10^6 points. Also plotted is Eq. (3).

eliminated, and the majority of remaining clusters will have a number of nodes too small to satisfy the elimination criteria. A good choice is to use a value close to unity: we found from our simulations that the best range for X_c is between 0.8 and 1.2, corresponding to the cumulative probabilities of 0.384 and 0.683, respectively. In fact, although the probability to find an edge smaller than $\sim \Lambda_m$ is still large, it is unlikely that a high number of these edges will belong to a single remaining cluster and they are therefore rejected by the subsequent filtering.

3.2 Distribution of the number of sub-trees for a given Λ_c in a random field

As shown by Di Gesù and Sacco (1983), the expected total number of clusters obtained by cutting a random, 2-dimensional MST having N_{tot} points, at an edge length Λ_c , is given by:

$$\bar{N} = 1 + (N_{\text{tot}} - 1) \exp\{-\pi\Lambda_c^2 N_{\text{tot}}/A\} \quad (5)$$

where N_{tot}/A is the density of nodes, that according Eq. (1) is proportional to $1/\Lambda_m^2$. This is a monotonic decreasing function, and we verified with Monte Carlo simulations the consistency of this result.

We used a different approach, directly based on the calculated mean edge length and considered another distribution, useful for selecting the best N_c parameter, that of the number of clusters as a function of the number of nodes after the application of a separation at the edge length Λ_c . We computed several distributions in random fields via Monte Carlo simulations and found that they can be well described by an exponential function:

$$T(N_n) = F(X_c) \cdot N_{\text{tot}} \cdot e^{-\kappa(X_c)N_n} \quad (6)$$

where $T(N_n)$ is the total number of sub-trees having N_n nodes each and $X_c = \Lambda_c/\Lambda_m$. Some examples, corresponding to different choices of the cut length Λ_c , are shown in Fig. 4. We see how the mean number of big clusters decreases when the cut length becomes smaller than the mean MST edge length: that is explained by the fact that separating at

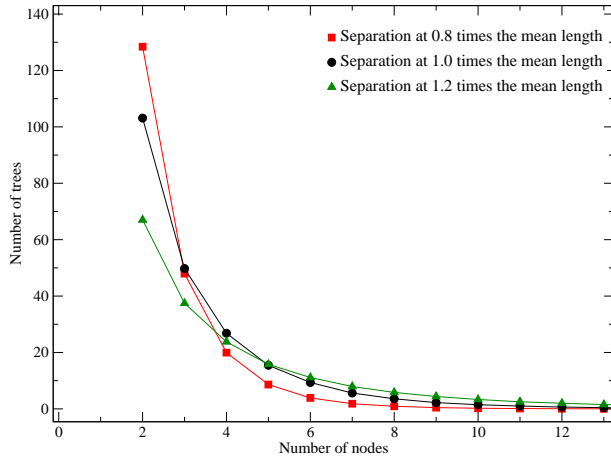


Figure 4. Average number of sub-trees obtained separating a 1000 points random field at 0.8, 1.0 and 1.2 times the mean MST length.

smaller lengths (thus removing more edges from the MST) we tend to “fragmentate” the tree in more small pieces.

Considering the MST of a field with a total number of points N_{tot} and applying a separation at Λ_c , we can establish an useful lower-limit for the elimination value N_c by comparing it with a random field with the same number of points and separated at the same length. A simple criterion is to choose the N_c value for which, in the corresponding random field, on average there is only one sub-tree with the same node number:

$$T(N_n) \leq 1 \Leftrightarrow N_c \geq N_c^1 = \frac{\ln(F(X_c) \cdot N_{\text{tot}})}{\kappa(X_c)} \quad (7)$$

Another possibility is to use the value N_c^* for which the expected number of residual casual clusters is less than unity, which is obtained by integrating the distribution of Eq.(5):

$$\int_{N_c^*}^{\infty} T(N_n) dN_n \leq 1 \Leftrightarrow N_c^* \geq N_c^1 - \frac{\ln \kappa(X_c)}{\kappa(X_c)} \quad (8)$$

Note that N_c^* is slightly greater than the value given by Eq. (7). Of course, the choice $N_c > N_c^*$ would give a higher confidence on the source detection, but the risk of eliminating true faint sources increases.

The two functions $F(X_c)$ and $\kappa(X_c)$ are characterized by a monotonic decreasing behaviour and are well described by the following power laws:

$$F(X_c) = 0.2 X_c^{-3.74} \quad (9)$$

and

$$\kappa(X_c) = 0.5 X_c^{-1.93} \quad (10)$$

In a random field we have $F(X_c) = 0.461, 0.200, 0.101$ and $\kappa(X_c) = 0.77, 0.50, 0.35$ for $X_c = 0.8, 1.0, 1.2$, respectively.

4 CLUSTERING PARAMETER AND DETECTION STABILITY

4.1 Clustering parameter

Once a list of candidate sources is found, it is useful to introduce some criteria to select, among the sub-trees remaining

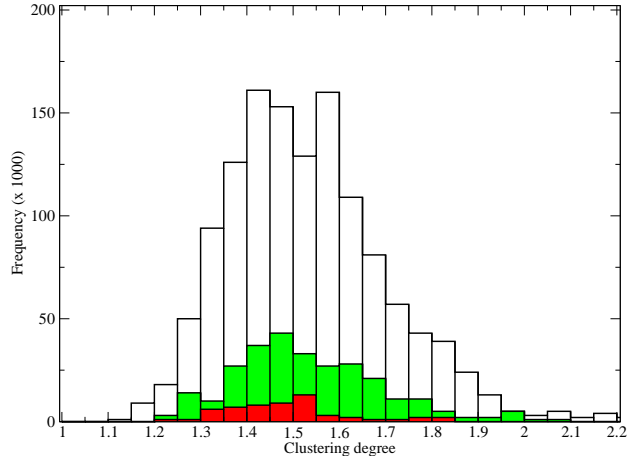


Figure 5. Frequency distribution of the clustering degree for the residual clusters, for $N_c = 12$ (white), 16 (green/light dark) and 20 (red/dark).

after the application of the filters, those corresponding to the best candidate sources and to reject clusters with a high chance to be randomly originated.

A first parameter is the “clustering degree” that we define as $g = \Lambda_m / \Lambda_{m,\text{tree}}$, i.e. the ratio between the mean edge length in the whole MST to the one of the edges in the sub-tree. The more clustered is a sub-tree (then, the more likely is the candidate source to be true), the less will be its mean edge length $\Lambda_{m,\text{tree}}$ and the bigger will be the value of the clustering degree g .

We tested how g works investigating its distribution for clusters in a random field. We generated 1000 fields of 1000 points each and evaluated g for the remaining clusters, after a separation at $\Lambda_c = \Lambda_m$ and elimination at $N_c = N_c^* = 12$. In Fig. 5 we show the histogram of the resulting distribution of g for the residual clusters, about one for each field as expected. It has an approximate Gaussian shape, although with asymmetric tails. The maximum is around $g = 1.5$ and the skewness has the low value of $\beta_3 \simeq 0.2$. An acceptable fit can be obtained by the same Pearson distribution used in Eq. (4), without the exponential suppression factor. For comparison, the distributions of g in which the elimination value is raised to $N_c = 16$ and 20 are also shown. It’s evident that the mean clustering degree of the residual clusters is still around $g = 1.5$, but the frequency of these clusters is much lower. We can conclude that, in a “true” field with the same number of points and separated at the same length, clusters with $g > 1.7$ combined with a number of nodes sufficiently higher than N_c^* , are good candidates to be genuine sources. For example, in our simulations, cutting respectively at $N_c = 12, 16$ and 20 we have frequencies of random clusters with $g > 1.7$ of about 20%, 4% and 0.5%, respectively. A higher threshold value of g would result in a safer rejection of spurious clusters, but in this case it is also possible to eliminate real weak sources. A good choice can be reached by comparing the values of g between the remaining clusters.

For the two clusters of Fig. 1 (lower-right panel) we have $g = 2.21$ and $g = 1.96$ for the “strong” and the “faint”

source, respectively, while lowering the N_c value below $N_c^* = 10$ spurious clusters also with $g > 1.7$ appear.

4.2 Bootstrap method and detection stability

We can define another parameter to take into account that the position of individual events in γ -ray images does not coincide with the true incoming direction of photons, because the typical uncertainty due to the reconstruction of pair trajectories is of the order of a few degrees. A γ -ray image, therefore, must be considered as a possible realisation of a large set of images of the “true” field in the sky. To take into account this effect and to verify if the detected clusters were produced by casual aggregation of events or can be considered associated with real sources, we introduced a “bootstrap” technique that can be used to improve the confidence on detections. Starting from the original image, we produce a set of other possible images by generating an equal number of photons whose coordinates are randomly extracted with a probability density function approximating the instrumental PSF, and including the energy dependence. We then apply the MST algorithm to these bootstrapped fields, with the same filter selection as in the original one, and as output we obtain new lists of candidate sources to be compared with the original detections. Those having positions within the PSF size are assumed to correspond to the same original source. Candidate sources having a high detection frequency in the bootstrapped images correspond to rich and dense clusters and have a high probability to be real, whereas sources characterised by a small number of nodes and a low clustering degree g are generally detected with a low frequency. The “detection stability” parameter s is then given by the ratio of the number of detections inside a source circle to the total number of bootstrapped fields. Sometimes a single cluster is divided into a couple of smaller clusters inside the source circle. In this cases, smaller sources are counted as a single detection to avoid that s can result higher than unity. From our simulations we found that one can consider a source detection as reliable if the corresponding cluster is detected in at least one half of the bootstrapped fields, i.e. with $s \geq 0.5$.

An example is given in Fig. 6, where we show a bootstrap of the Fig. 1 field. In the upper left panel the original field is shown, while the upper right panel is a bootstrapped field computed using a probability density function equal to the one used to generate the simulated sources, i.e. a Gaussian with $\sigma = 0.1$. Note that the strong source is more or less unaffected by the redistribution of photons, whereas some other small clusters appear, but they are rejected by further filtering. In the lower panels the clusters remaining after the MST application (left: $\Lambda_c = 1.3 \Lambda_m$, $N_c = 7$, right: $\Lambda_c = \Lambda_m$, $N_c = 10$) onto this particular bootstrapped field: note the different shape and number of clusters with respect to the corresponding panels in Fig. 1. With the generation of 100 bootstrap fields and the first selection of filters, we obtain a detection stability of $s = 1$ for both sources. If we choose the second set of filters the detection stability is $s = 1$ and $s = 0.55$ for the “strong” and the “faint” source, respectively.

The bootstrap method can also be used when the MST algorithm detect two very close clusters, with a separation between the centroids less than the PSF size, an effect likely

due to the presence of an edge just above the cutting threshold. In this case a large fraction of the bootstrapped fields has a single cluster at the position of these two sub-trees and we can conclude that the splitting into two clusters was accidental and that they correspond to a unique source.

The statistical distribution of the expected values of s in a random field cannot be computed because it depends upon the instrumental response functions used when bootstrapped coordinates are generated. An estimate of the threshold s value to reject unstable clusters must be then obtained from a comparison of the resulting values. We also noticed in our simulations that the source position computed averaging the centroids of the bootstrap replicas is frequently, although not always, closer to the actual source location than that derived from the MST application to the original field. Eventually, this method can be also used to refine the source coordinates.

5 APPLICATION OF MST TO EGRET FIELDS

To test the source detection capability of our implementation of the MST, we applied it to a real γ -ray image in which several sources were already found. Due to the simplicity of our algorithm (for example, we don’t treat the energy dependence of the point-spread function and the geometrical distortions of photon distribution in a flat projection), we choose an high galactic latitude field in order to have a low, uniform background, with no strong intensity gradient. Moreover, this field lies around the celestial equator and projection effects on photon coordinates are negligible, being smaller than a few percent.

Fig. 7 shows the central portion of the EGRET Cycle 1 VP-11.0 field for photon energies higher than 100 MeV³, observed between 03 and 17 October 1991 and comprising the quasars 3C 273, 3C 279 and other sources. In the left panel, blue squares mark the sources detected in this specific pointing and reported in the Third Egret Catalog (3EG, Hartman et al. 1999), while the red squares are other 3EG sources in field but not detected in this pointing (i.e. only upper limits on the flux are given in the catalog).

A first application of MST, using the filtering parameters $\Lambda_c = 0.9 \Lambda_m$ and $N_c^* = 12$, gave the detection of 10 clusters, shown as black circles in the same figure. We then used the bootstrap method (see Sect. 4) sorting new photon directions with a Gaussian distribution centered at each original point and having a $\sigma = 2^\circ$. Note that *a*) the choice of a Gaussian distribution for the bootstrapped photons is a simplified and energy-averaged approximation of the instrumental PSF, and *b*) the use of a circle for the computation of s is only a zeroth-order approximation of the actual photon distribution, that for real astronomical data would be rather an ellipse, due to geometrical projection effects. Over 100 bootstrap fields were so produced, and only the seven candidate sources with a clustering degree $g > 1.70$ and with a detection stability $s > 0.5$ were retained. The MST detected clusters satisfying these criteria are given in Fig.

³ A standard energy-dependent cut on zenith angle has been applied to the original photon list, in order to remove Earth albedo γ -ray background (Esposito et al. 1997).

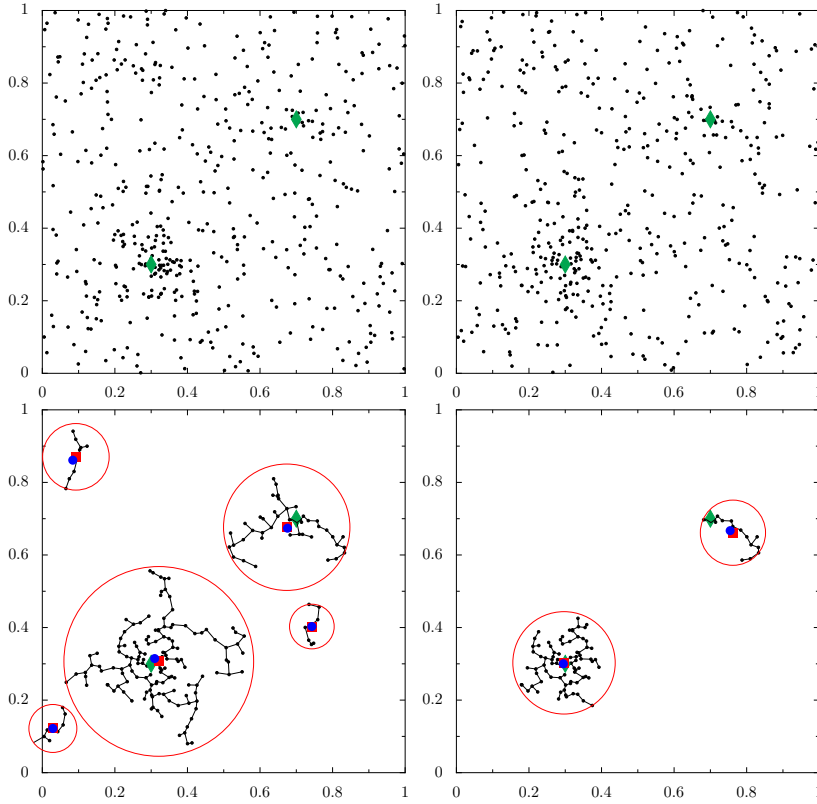


Figure 6. *Upper left:* The 500-point field of Fig. 1, with two simulated sources. *Upper right:* A bootstrap realisation of the same field, with $\sigma = 0.1$. *Lower left:* Cluster selection after the applications of the filters $\Lambda_c = 1.3 \Lambda_m$ and $N_c = 7$ onto the bootstrapped field. *Lower right:* Cluster selection after $\Lambda_c = \Lambda_m$ and $N_c = 10$ onto the bootstrapped field. The meaning of symbols is the same as in Fig. 1.

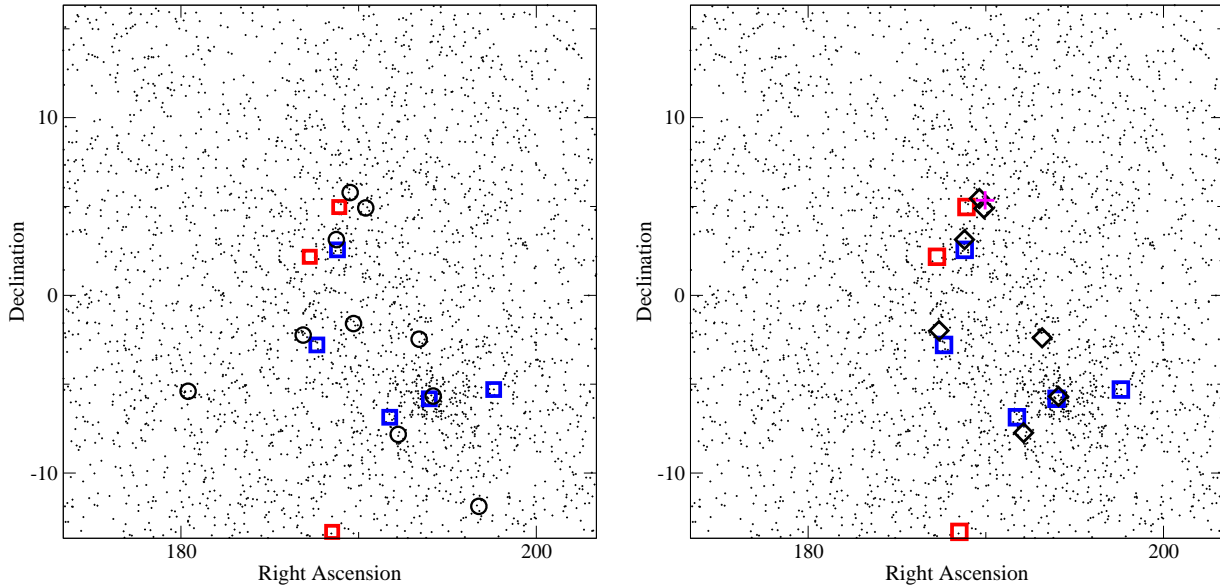


Figure 7. *Left:* EGRET-VP11.0 pointing, $30^\circ \times 30^\circ$ square field, centered on RA 188.38, DEC +1.33. Blue/dark squares are the 3EG sources detected in this pointing, red/light dark squares the other 3EG sources within this area. Black circles are the MST-detected candidate sources. *Right:* The black diamonds are the positions of candidate sources calculated via the bootstrap method. Only the sources with a clustering degree $g > 1.70$ and with a bootstrap detection stability $s > 0.5$ are retained. The cross here mark the mean coordinates of the two clusters that likely belong to the same source, see text for discussion.

7 (right panel) and Table 1, where we report the coordinates, number of nodes, the clustering degree g , bootstrap detection stability s , the 3EG counterpart and the possible identification based on the new catalogue of blazars Roma-BZCat (Massaro et al. 2005).

For this pointing, the 3EG catalogue reports five sources, while two other sources are detected in other pointings of the same field. Five of these seven 3EG sources were also detected by the MST method and their angular distance from the catalog positions is $\sim 1^\circ$ or less. Four correspond to the 3EG sources detected in this pointing, while the fifth, 3EG J1310-0517, which is reported as an unidentified and possibly confused source, is not detected (although there is a 12-node cluster that correspond to this source after the separation, thus just below the elimination value). We found also some additional clusters. Two of them (RA=189.52°, $\delta=5.78^\circ$; RA=190.40°, $\delta=4.92^\circ$) have the small separation of $\sim 1^\circ$ and lie close 3EG J1236+0457, which was not detected in this pointing by Hartman et al. (1999). The distance between their centroids is less than the PSF radius, so it is very likely that they belong to a single source: the sub-tree of this source was split into two sub-trees by removing one single edge having a length slight exceeding Λ_c . This is confirmed by the fact that in about one half of the bootstrapped fields there is a single cluster near this position. For this reason we can consider the two clusters as belonging to a unique source located approximately at the mean position (RA=189.96°, $\delta=5.35^\circ$). This source is likely associated with the $z = 1.762$ flat spectrum radio quasar BZQ J1239+0443. We investigated whether in other EGRET pointings containing the same region of the sky this source is present, and detected it in VP-408.0 and VP-306.0. In the former pointing the source was also detected by Hartman et al. (1999), but not in the latter. Although, we didn't find it in VP-407.0 where it was reported by Hartman et al. (1999). This discrepancy is to be attributed mainly to the faintness of these sources, which make the detection extremely sensitive to the actual source detection method used and its threshold values.

MST algorithm detected a cluster at the coordinates (RA=193.41°, $\delta=-2.47^\circ$), which is not in the 3EG catalogue. In particular, this cluster has MST parameters comparable to those of 3C 273 and there is no reason to reject it. We searched without success in the Roma-BZCat and in the NED database for possible counterparts and therefore it remains unidentified. Of course, the possibility that it must not be considered genuine and originated by random clustering of events in the field cannot be excluded.

6 DISCUSSION

We presented an application of a Minimal Spanning Tree algorithm to the problem of source detection in γ -ray images. This method does not involves in the computation the instrumental response functions and works recognizing the regions of the sky where arrival directions of photons clusterize. It has the advantages of a fast calculation but did not provide directly estimates of the source flux. We have shown that a MST based algorithm is a viable method to detect γ -ray sources both in simulated images and in real γ -ray observations of the EGRET experiment on board Compton-

GRO. We proposed some tools to optimize the filtering parameters and to assess the reliability of source detections, like the clustering degree and the bootstrap detection stability. These tools are based on a study, although empirical, of the statistical properties of the Minimal Spanning Tree on random fields.

The MST application to an EGRET field around the two famous γ -ray loud quasars 3C 273 and 3C 279 found almost all the 3EG sources already detected in the same pointing and confirmed the presence of another source, detected in a different pointing. We consider this result a good indication that MST method is particularly efficient. We found also evidence of a new possible source with a significance comparable to that of other well established sources. We expect that future experiments with a better sensivity, like the LAT instrument on board GLAST, will confirm or disprove this finding.

There are, however, several possible effects that make difficult the source detection and require even more attention when the MST method is used. These problems can be divided into four main categories: *i*) problems due to the presence of strong sources, *ii*) problems arising from energy spectra of the sources different from that of the background; moreover, different spectral indices between the sources will result in different probabilities to be detected, due to the energy dependence of the PSF, *iii*) problems originated by images with a non-homogeneous background, *iv*) problems due to the geometrical distortions from the arriving celestial photons in projection onto the γ -ray telescope, that will result not necessarily in a circular shape to characterize proper cluster selections. At present we have not developed a well established strategy to solve these problems and in the following we will briefly discuss some aspects useful for the understanding of results.

One or more strong sources in the field have various possible consequences. A first relevant effect is that they are characterized by a high clustering degree and consequently reduce the value of Λ_m with respect to the one expected in the field if they were absent. A value of Λ_c very close to Λ_m would here be good to detect strong sources but this selection criterion could miss other possible sources of lower flux. Another effect is the presence of possible "satellites" in the surroundings of a strong source, even closer than expected from the PSF, originated by cutting an edge whose length is just smaller than Λ_c . For example, the cluster detected in the EGRET field (see Sect. 4) with no obvious counterpart, is at a distance of about 3.3° from the strong radio quasar 3C 279, and therefore we cannot exclude that it could be a satellite of the latter. Usually, the satellites do not have a high frequency in the bootstrap fields.

The energy distribution of the photons also affects the source detection, because the PSF of γ -ray telescopes changes with the energy becoming much narrower at high energies. This implies that sources with spectra harder than the background are better detected in high energy images because their clustering degree increases. At variance, sources with soft spectra give more disperse clusters and cannot be easily found.

Another class of problems is present when the background is markedly non-homogeneous, as in the case where the field contain a portion of the galactic disc. In this case, using an unique Λ_c in all the image would correspond to a

Table 1. MST-detected clusters in EGRET pointing 110.0, with $g > 1.7$ and $s > 0.5$. For each candidate source are reported the celestial coordinates (Right Ascension and Declination, in degrees), the number of nodes of the relative cluster, the clustering degree g , the bootstrap detection stability s , the Third EGRET Catalog (3EG) counterpart, and the identification with known sources.

RA	DEC	N_n	g	s	3EG counterpart	Identification
194.20	-5.66	201	2.31	1.	3EG J1255-0549	3C 279
193.41	-2.47	21	1.88	1.	—	—
192.22	-7.82	37	1.83	1.	3EG J1246-0651	BZB J1243-0613
190.40	4.92(*)	16	1.79	1.	3EG J1236+0457	BZQ J1239+0443
188.75	3.14	23	1.71	1.	3EG J1229+0210	3C 273
189.52	5.78(*)	17	1.71	1.	3EG J1236+0457	BZQ J1239+0443
186.88	-2.23	15	2.35	0.92	3EG J1230-0247	BZQ J1236+0224

(*) These two clusters likely correspond to a unique source, located at about (189.96, 5.35), as indicated by the fact that their clusters are connected in about half of bootstrapped fields.

long cutting in the dense region and to a short cutting in the region of low density with the consequence of missing real sources and producing more spurious clusters.

A general approach to be used for γ -ray source detection is that of using several methods, possibly based on different techniques, and to compare their results. In this way it will be possible to reduce the number of spurious detections, because of the different criteria and *a priori* assumptions applied in the source recognition. Accordingly, MST method can be used to obtain a quick list of photon clusterization regions, that could correspond to possible sources, to be studied independently with other methods.

There are other clustering algorithms that can be applied to γ -ray source detection, like the Voronoi tessellation (Icke & van de Weygaert 1987, Aurenhammer 1991). In particular, this method is based on the construction of its dual graph, the Delaunay triangulation, of which MST is a subset. We think, therefore, that at least in principle, they would provide similar result and that a combined figure of merit for source detection should be defined.

Here we discussed gamma-ray astronomy as a prime candidate for the application of MST method, but it could be even better applicable to the study of data clusterization in ultra-high energy cosmic rays (UHECR) and hemispherical neutrino experiments, that are characterized to the absence of structured background. We think also that it will be possible to extend MST to higher dimensional spaces introducing time and energy as additional dimensions. Basically there are two approaches: *i*) to search for clusters in separate, dimensionally homogeneous subspaces, and then to search for the intersection of the detected clusters and *ii*) to define a new metric for the tree edges that combine together the various dimensions in a suitable way for the MST computation. Preliminary numerical attempts based on the second approach, with energy as third coordinate, seem to be very promising to identify sources having spectra different from that of the background. Another possible 3-dimensional generalization is to take into account also the time, thus searching for variable or stable sources. We will discuss a possible application of such a generalized MST in a subsequent work.

ACKNOWLEDGMENTS

We are grateful to Cettina Maccarone, Bruno Sacco, Paolo Giommi and Gino Tosti for useful discussions. We also thank the anonymous referee for insightful comments. This work is partially supported by ASI-INAF funds for the scientific programs with GLAST.

REFERENCES

Aurenhammer F., 1991, ACM Computing Surveys, 23, 345-405
 Barrow J. D., Bhavsar S. P., and Sonoda D. H., 1985, MNRAS, 216, 17-35
 Bennett K., 1990, Nuc. Phys. B (Proc. Suppl), 14B, 23-34
 Bhavsar S. P., Ling E. N., 1988a, PASP, 100, 1314-1319
 Bhavsar S. P., Ling E. N., 1988b, ApJL, 331, L63-L68
 Damiani F., Maggio A., Micela G., Sciortino S., 1997, ApJ, 483, 350-369
 De Biase G. A., Di Gesù V., Sacco B., 1986, Pattern Recognition Letters, 4, 39-44
 Delaunay B., 1934, Izvestia Akademii Nauk SSSR, 7, 793-800
 Di Gesù V., Sacco B., 1983, Pattern Recognition, 16, 525-531
 Di Gesù V., Maccarone M. C., 1986, Pattern Recognition, 19, 63-72
 Doroshkevich A., Tucker D. L., Fong R., Turchaninov V., Lin H., 2001, MNRAS, 322, 369-388
 Doroshkevich A., Tucker D. L., Allam S., Way M. J., 2004, A&A, 418, 7-23
 Esposito J. A., et al., 1997, ApJSS, 123, 203-217
 Fichtel C.E., et al., 1975, ApJ, 198, 163
 Gilbert E. N., 1965, Journ. Soc. Ind. Appl. Math., 13, 376-387
 Gehrels N., et al., 1999, Astropart. Phys., 11, 277-282
 Hartman, R. C., et al., 1999, ApJS, 123, 79-202
 Herranz D., Sanz J. L., Barreiro R. B., Martinez-Gonzales E., 2002, ApJ, 580, 610-625
 Icke V., van de Weygaert R., 1987, A&A, 184, 16-32
 Kanbach, G., et al., 1988, Space Sci. Rev., 49, 69-84
 Kruskal J. B., 1956, Proc. Am. Math. Soc., 7, 48
 Krzevina L. G., Saslaw W. C., 1996, MNRAS, 278, 869-876
 Massaro E., Sclavi S., Giommi P., Perri M., Piranomonte S., 2005, Multifrequency Catalogue of Blazars, Aracne, <http://www.asdc.asi.it/bzcat/>

- Mattox, J. R., et al., 1996, ApJ, 461, 396-407
Plionis M., Valdarnini R., Jing Y. P., 1992, ApJ, 398, 12-32
Prim R. C., 1957, Bell System Tech. J., 36, 1389
Sanz J. L., Herranz D., Martinez-Gonzalez E., 2001, ApJ, 552, 484-492
Smart W. M., 1958, Combination of Observations, Cambridge University Press
Tavani, M., et al., 2006, Proc. of SPIE, 6266, 626603
Thompson, D. J., et al., 1993, ApJS, 86, 629-656
Zahn C. T., 1971, IEEE Trans. on Computers, C20, 68